Adv. Manuf. (2014) 2:295–302
DOI 10.1007/s40436-014-0094-x

Kinematic analysis and simulation of a new-type robot with special structure

Shuai Guo · Hua-Wei Li · Jian-Cheng Ji · Zhi-Fa Ming

Received: 12 March 2014 / Accepted: 6 November 2014 / Published online: 7 December 2014
© Shanghai University and Springer-Verlag Berlin Heidelberg 2014

Abstract Common methods, such as Denavit-Hartenberg (D-H) method, cannot be simply used in kinematic analysis of special robots with hybrid hinge as it is difficult to obtain the main parameters of this method. Hence, a homogeneous transformation theory is presented to solve this problem. Firstly, the kinematics characteristic of this special structure is analyzed on the basis of the closed-chain theory. In such a theory, closed chains can be transformed to open chains, which makes it easier to analyze this structure. Thus, it will become much easier to establish kinematics equations and get the solutions. Then, the robot model can be built in the Simmechanics (a tool box of MATLAB) with these equation solutions. It is necessary to design a graphical user interface (GUI) for robot simulation. After that, the model robot and real robot will respectively move to some spatial points under the same circumstances. At last, all data of kinematic analysis will be verified based on comparison between data got from simulation and real robot.

Keywords Mixed hinge structure · Homogeneous transformation · Kinematic analysis · Kinematic simulation

1 Introduction

Usually, we use Denavit-Hartenberg (D-H) method to analyze the kinematics of robot. The key of this method is to establish a set of D-H parameters which indicate the relationship of the coordinate systems of all joints [1]. There are a lot of studies on the serial chain industry robots, however few studies are on such industry robots with complex structures. For example, a kind of large universal industry robot with hybrid hinge structure allows its arm to move backwards in low energy consumption. The motion law of this robot differs from that of other robots and its D-H parameters cannot be determined easily. Two solutions are proposed to deal with this special structure. One is to transform the structure into equivalent serial joints (revolute or prismatic joints). Then we can determine the D-H parameters one by one based on D-H theory [2]. The other is to transform closed chains to open chains so that we can calculate the relationship between the active and passive joints. Then, the complex structure is transformed into simple serial structure [3]. The first method needs to analyze the characteristics of every joint in this hybrid hinge, thus it is sophisticated and error-prone [4]. Meantime, in the second method, although a general theory to analyze all closed chains is introduced, the breakdown structure is not presented and this theory is not verified by experiments. Considering these two methods, it will be easier for us to determine the relationship between coordinate systems of joints if we know the kinematics characteristic of the special structure. Hence the motion characteristic of the special structure is analyzed based on the closed-to-open chain theory in the paper. Then the coordinate systems are directly established at each active joint. The advantage of the method is that it can avoid judging the motion of each kinematic pair in the structure [5]. In addition, it is convenient to build the simulation model mentioned below.

S. Guo (✉) · H.-W. Li · J.-C. Ji · Z.-F. Ming
Key Laboratory of Intelligent Manufacturing and Robotics, School of Mechatronics Engineering and Automation, Shanghai University, Shanghai 200444, People's Republic of China
e-mail: guoshuai@shu.edu.cn

2 Kinematics characteristic of new-type robot

Figure 1 shows the large universal robot—ZX165U of Kawasaki Company. Such robots can keep the translation

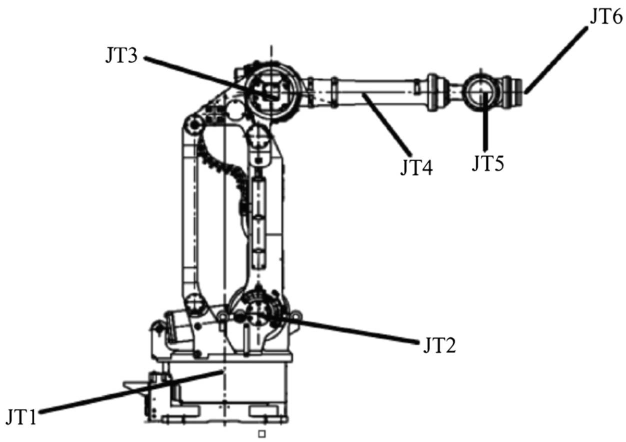

Fig. 1 Industry robot consisting of hybrid hinge structures

motion of its end-effector when it is palletizing. During this process, fewer motors work, thus less energy is consumed. Furthermore, the damper settled on the base is an important component to keep the object stable and safe in the whole process [6]. All joints except the joint 2 (JT2) are the same as those in usual robots. In this paper, we will only discuss how the spinning of joint 2 affects the kinematics characteristic of the whole robot [7, 8].

Firstly, we theoretically analyze the kinematics characteristic of the special structure. Figure 2a demonstrates a mixed system consisting of closed chain structure. There are n links and L_i is the name of a certain mid-link in the system. Figures 2b, c are two kinds of logic open-chain systems generated from Fig. 2a. The producing mode of these two open-chain systems is shown as following [3, 9]. All links with which the closed chain intersects with outside world are determined (such as L_m and L_{m+4} in Fig. 2a). And then all parallel links connected to these links (L_m and L_{m+4}) are figured out. Thus we can easily choose two different routes (from L_m to L_n), where no parallel link exists. Finally, two logic open-chain systems are generated according to corresponding selected routes. As a result, all non-redundant links exist in the logic open-chain systems, as shown in Figs. 2a, b.

Considering the characteristic of the robot we are studying, there are totally 8 links. So n will be equal to 8 if m is equal to 1 (see Fig. 2). The degree of freedom (DOF) (N) is equal to 6 (the number of active joints), and the number of passive joints (P) is equal to 3. We assume the variables of the active joints as $q_{\mathrm{A},i}$ ($i = 1, 2, \cdots, 6$) and the variables of the passive joints as $q_{\mathrm{P},j}$ ($j = 1, 2, 3$). In the theoretical basis and research scope of rigid body dynamics, rigid displacement is only determined by the six active joints exclusively [10]. The relative equation is

$$q_{\mathrm{P},j} = q_{\mathrm{P},j}\left(q_{\mathrm{A},1}, q_{\mathrm{A},2} \cdots, q_{\mathrm{A},6}\right), \quad j = 1, 2, 3. \tag{1}$$

Equation (1) shows the displacement dependency between passive and active joints, which can be written as

$$q_{\mathrm{P},j} = q_{\mathrm{P},j}(q_1, q_2, \cdots, q_9), \quad j = 1, 2, 3. \tag{2}$$

There are other two geometric constraints. One is that link L_{m+1} is fixed on the base. The other is that the closed chain is a parallelogram structure. Consequently, from Eq. (2) we can obtain

$$-q_4 = -q_5 = q_3 = q_2. \tag{3}$$

Namely, the L_{m+2} moves the same as the L_{m+3} does. So the manipulator fixed on the link L_{m+5} keeps executing translation consistently.

Figure 3 shows the simulation model of the robot. Only the joint 2 is rotating in the simulation process. Figure 3a shows the initial state of the robot meaning that all the angles of joints are 0. Figures 3b, c demonstrate the corresponding status of the robot when the joint 2 moves π/4 clockwise and anticlockwise respectively. The manipulator keeps translation motion all the time, which is consistent with the actual situation (see Fig. 3).

Now, we can make a conclusion that the end-effector of the robot executes translation motion while all joints are fixed except the rotating joint 2.

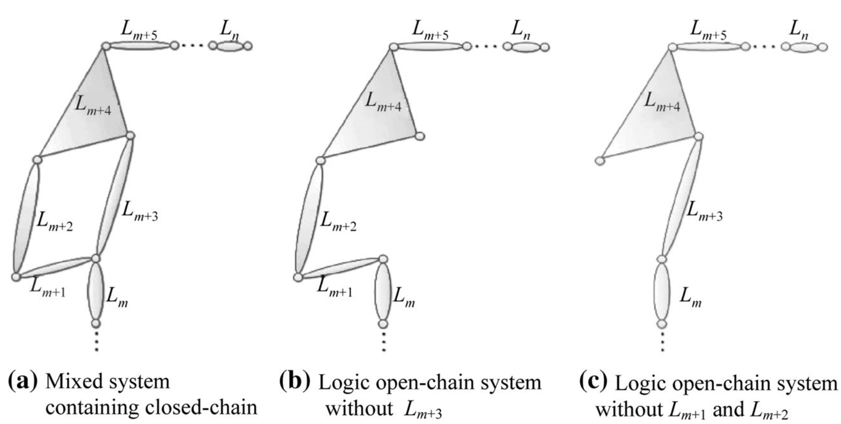

Fig. 2 Closed-chain system and open-chain systems

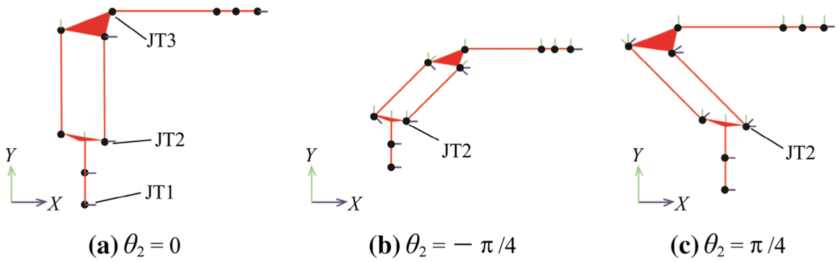

Fig. 3 Motion status of robot manipulator when only JT2 moves to 0, $-\pi/4$ and $\pi/4$

3 Kinematics analysis

The aim of kinematics analysis is to describe the kinematic relationship between joints and end-effector. The analysis solutions can demonstrate how to control robot motion, and establish the dynamic equation and the model for error analysis [11, 12].

3.1 Forward kinematics and homogeneous transformation

The position of joints and orientations of rigid bodies can be described by coordinate systems fixed on joints [10]. So we build coordinate system on every active joint [12].

In Fig. 4, the coordinate system of ZX165U robot is established. First of all, the coordinate system 1 is established and it coincides with the base coordinate system 0. For convenience, the Z axis is parallel to the axis of each rotating joint and the direction of Z axis is determined by the rotation direction and fixed conventionally by right hand rule. The second axis is exactly consistent with one of the certain axes in previous coordinate system. Finally, the last axis is determined by the right hand rule again.

The dimension parameters in the coordinate system are shown in Fig. 4, in which the axes Z_1–Z_6 are consistent with the revolute joints JT1–JT6, $L_1 = 670$ mm, $L_3 = 1\ 100$ mm, $L_4 = 270$ mm, $L_5 = 288$ mm, $L_6 = 1\ 100$ mm, $L_7 = 228$ mm.

According to homogeneous transformation formula

$$
{}^{i-1}_{\ \ i}\boldsymbol{T} = \left[\begin{array}{ccc|c} & {}^{i-1}_{\ \ i}\boldsymbol{R} & & \boldsymbol{D} \\ \hline 0 & 0 & 0 & 1 \end{array}\right], \tag{4}
$$

we can obtain all matrices: ${}^{0}_{1}\boldsymbol{T}$, ${}^{1}_{2}\boldsymbol{T}$, ${}^{2}_{2t}\boldsymbol{T}$, ${}^{2t}_{3t}\boldsymbol{T}$, ${}^{3t}_{3}\boldsymbol{T}$, ${}^{3}_{4}\boldsymbol{T}$, ${}^{4}_{5}\boldsymbol{T}$, ${}^{5}_{6}\boldsymbol{T}$, ${}^{6}_{e}\boldsymbol{T}$. The character "e" represents end-effector coordinate; ${}^{i-1}_{\ \ i}\boldsymbol{T}$ refers to the transformation relationship from the coordinate $i-1$ to i; ${}^{i-1}_{\ \ i}\boldsymbol{R}$ refers to the revolution relationship from the coordinate $i-1$ to i; $\boldsymbol{D}$ refers to the translation vector from the coordinate $i-1$ to i. In Fig. 4, for example, coordinate system 1 shifts L_2 distance along the $+Y$, and shifts L_1 distance along the $+Z$, then anticlockwise rotates $\pi/2$ around the $+Y$. Then it can be transformed to coordinate 2. The transformation matrix is

$$
{}^{1}_{2}\boldsymbol{T} = \boldsymbol{T}_Z(L_1)\boldsymbol{T}_Y(L_2)\boldsymbol{R}_Y(\pi/2), \tag{5}
$$

where $\boldsymbol{T}_Z(L_1)$ and $\boldsymbol{T}_Y(L_2)$ refer to translation matrices; L_1 and L_2 are translation lengths along the corresponding axes; $\boldsymbol{R}_Y(\theta)$ refers to rotation matrix; θ is anticlockwise rotation angle around the $+Y$.

When other matrices are computed, the transformation matrix from end-effector coordinate to base coordinate is obtained [13, 14]. The solution to the forward kinematics is as follows

$$
{}^{0}_{e}\boldsymbol{T} = {}^{0}_{1}\boldsymbol{T}{}^{1}_{2}\boldsymbol{T}{}^{2}_{2t}\boldsymbol{T}{}^{2t}_{3t}\boldsymbol{T}{}^{3t}_{3}\boldsymbol{T}{}^{3}_{4}\boldsymbol{T}{}^{4}_{5}\boldsymbol{T}{}^{5}_{6}\boldsymbol{T}{}^{6}_{e}\boldsymbol{T} = \begin{bmatrix} n_x & o_x & a_x & p_x \\ n_y & o_y & a_y & p_y \\ n_z & o_z & a_z & p_z \\ 0 & 0 & 0 & 1 \end{bmatrix}, \tag{6}
$$

where

$$
\begin{aligned}
n_x &= c_6(c_1c_4 - s_1s_3s_4) - s_6(c_5(c_1s_4 + c_4s_1s_3) + c_3s_1s_5), \\
n_y &= c_6(c_4s_1 + c_1s_3s_4) - s_6(c_5(s_1s_4 - c_1c_4s_3) - c_1c_3s_5), \\
n_z &= s_6(s_3s_5 - c_3c_4c_5) - c_3c_6s_4, \\
o_x &= -c_6(c_5(c_1s_4 + c_4s_1s_3) + c_3s_1s_5) - s_6(c_1c_4 - s_1s_3s_4), \\
o_y &= -c_6(c_5(s_1s_4 - c_1c_4s_3) - c_1c_3s_5) - s_6(c_4s_1 + c_1s_3s_4), \\
o_z &= c_6(s_3s_5 - c_3c_4c_5) + c_3s_4s_6,
\end{aligned}
$$

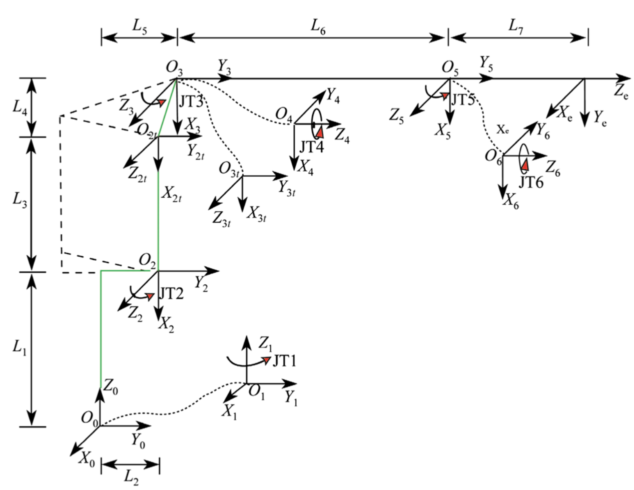

Fig. 4 Homogeneous coordinate system of Kawasaki ZX165U

$$
\begin{aligned}
a_x &= s_5(c_1 s_4 + c_4 s_1 s_3) - c_3 c_5 s_1,\\
a_y &= s_5(s_1 s_4 - c_1 c_4 s_3) + c_1 c_3 c_5,\\
a_z &= c_5 s_3 + c_3 c_4 s_5,\\
p_x &= L_3 s_1 s_2 - L_6 c_3 s_1 - L_5 s_1 - L_7 c_3 c_5 s_1 + L_7 c_1 s_4 s_5\\
&\quad + L_7 c_4 s_1 s_3 s_5,\\
p_y &= L_5 c_1 + L_6 c_1 c_3 - L_3 c_1 s_2 + L_7 c_1 c_3 c_5 + L_7 s_1 s_4 s_5\\
&\quad - L_7 c_1 c_4 s_3 s_5,\\
p_z &= L_1 + L_4 + L_3 c_2 + L_6 s_3 + L_7 c_5 s_3 + L_7 c_3 c_4 s_5,
\end{aligned} \tag{7}
$$

where $s_i = \sin\theta_i$, $c_i = \cos\theta_i$, $s_{ij} = \sin(\theta_i + \theta_j)$, $c_{ij} = \cos(\theta_i + \theta_j)$, $i, j = 1, 2, \cdots, 6$.

3.2 Inverse kinematics

The issue of robot inverse kinematics is to calculate all the corresponding joint angles when the pose and location of robot are given [13]. In other words, the joint variables θ_i ($i = 1, 2, \cdots, 6$) can be determined based on kinematics equation if the values of n, o, a, p and the needed geometric parameters are known [14]. Equation (7) is used to get the solution to the inverse kinematics equation. This paper determines the first three joint variables θ_i ($i = 1, 2, 3$) by means of algebraic method, and the common inverse transformation method [15] is used to determine the last three joint variables θ_i ($i = 4, 5, 6$).

First of all, there is only θ_1 left and other variables are eliminated by elimination method [16, 17] for Eq. (7), such as

$$p_x - L_7 a_x = -s_1(L_5 + L_6 c_3 - L_3 s_2), \tag{8}$$

$$p_y - L_7 a_y = c_1(L_5 + L_6 c_3 - L_3 s_2), \tag{9}$$

$$p_z - L_1 - L_4 - L_7 a_z = L_3 c_2 + L_6 s_3. \tag{10}$$

Assume

$$A = L_5 + L_6 c_3 - L_3 s_2. \tag{11}$$

Equation (11) is substituted back into Eqs. (8) and (9). Thus Eq. (12) is obtained.

$$
\begin{cases}
A^2 = (p_x - L_7 a_x)^2 + (p_y - L_7 a_y)^2,\\
\sin\theta_1 = -(p_x - L_7 a_x)/A,\\
\cos\theta_1 = (p_y - L_7 a_y)/A,\\
\tan\theta_1 = -(p_x - L_7 a_x)/(p_y - L_7 a_y),
\end{cases} \tag{12}
$$

therefore,

$$\theta_1 = \arctan\left(-(p_x - L_7 a_x)/(p_y - L_7 a_y)\right), \theta_1 \in [-2\pi, 2\pi]. \tag{13}$$

In Eqs. (10) and (11), the quadratic components of both sides are added together, and we get

$$A\sin\theta_2 - B\cos\theta_2 = C, \tag{14}$$

where $B = p_z - L_1 - L_4 - L_7 a_z, C = L_6^2 - (L_3^2 + L_5^2 - 2L_5 A + A^2 + B^2)/2L_3$.

Substituting $\sin\varphi = A$ and $\cos\varphi = B$ into Eq. (14) leads to

$$
\begin{cases}
D\cos(\theta_2 + \varphi) = C,\\
D = \sqrt{A^2 + B^2}.
\end{cases} \tag{15}
$$

Thus,

$$\theta_2 = \arccos(C/D) - \varphi, \theta_2 \in [-\pi/3, 5\pi/12]. \tag{16}$$

We can substitute θ_2 into Eqs. (10) and (11) and obtain

$$
\begin{aligned}
&\theta_3 = \arctan\left((B - L_3 \times \cos\theta_2)/(A + L_3 \sin\theta_2 - L_5)\right),\\
&\quad \theta_3 \in [-2\pi/3, 25\pi/18].
\end{aligned} \tag{17}
$$

Also θ_4, θ_5, θ_6 are determined as follows.

Equation (18) is deducted by multiplying both sides of Eq. (6) with all inverse transformation matrices from joint 1 to joint 3,

$${}^{3t}_{3}\boldsymbol{T}^{-1}\,{}^{2t}_{3t}\boldsymbol{T}^{-1}\,{}^{2}_{2t}\boldsymbol{T}^{-1}\,{}^{1}_{2}\boldsymbol{T}^{-1}\,{}^{0}_{1}\boldsymbol{T}^{-1}\,{}^{0}_{e}\boldsymbol{T} = {}^{3}_{4}\boldsymbol{T}\,{}^{4}_{5}\boldsymbol{T}\,{}^{5}_{6}\boldsymbol{T}\,{}^{6}_{e}\boldsymbol{T}. \tag{18}$$

So we get the equation below:

$$
\begin{bmatrix}
n_{3x} & o_{3x} & a_{3x} & p_{3x}\\
n_{3y} & o_{3y} & a_{3y} & p_{3y}\\
n_{3z} & o_{3z} & a_{3z} & p_{3z}\\
0 & 0 & 0 & 1
\end{bmatrix}
=
\begin{bmatrix}
c_6 s_4 + c_4 c_5 s_6 & c_4 c_5 c_6 - s_4 s_6 & -c_4 s_5 & -L_7 c_4 c_5\\
s_5 s_6 & c_6 s_5 & c_5 & L_6 + L_7 c_5\\
c_4 c_6 - c_5 s_4 s_6 & -c_4 s_6 - c_5 c_6 s_4 & s_4 s_5 & L_7 s_4 s_5\\
0 & 0 & 0 & 1
\end{bmatrix}. \tag{19}
$$

The left part of Eq. (19) contains known joint variables i.e., θ_1, θ_2 and θ_3, while the other side contains the joint variables θ_4, θ_5 and θ_6 to be solved. As a result,

$$
\begin{cases}
c_5 = a_z s_3 + a_y c_1 c_3 - a_x s_1 s_3,\\
\theta_5 = \arccos\left(a_z s_3 + a_y c_1 c_3 - a_x s_1 c_3\right),\\
\qquad \theta_5 \in [-13\pi/18, 13\pi/18].
\end{cases} \tag{20}
$$

Get rid of the singular solution, $\theta_5 = 0$,

$$
\begin{cases}
-c_4 s_5 = s_3 c_1 a_y - s_3 s_1 a_x - c_3 a_z,\\
\theta_4 = \arccos\left((c_3 a_z - s_3 c_1 a_y + s_3 s_1 a_x)/s_5\right), \theta_4 \in [-2\pi, 2\pi],\\
\theta_6 = \arccos\left((s_3 o_z + c_3 c_1 o_y - c_3 s_1 o_x)/s_5\right), \theta_6 \in [-2\pi, 2\pi].
\end{cases} \tag{21}
$$

4 Analysis of simulation

Model simulation can verify the correctness of the kinematic analysis, and provide intuitive understanding and rigorous data [1, 18]. The robot model discussed in this paper is built relying on the powerful function of the MATLAB platform.

4.1 The toolbox and the model

There are two qualified requirements [19, 20]. The first one is to build an accurate robot model. The second one is to control the model for communication. With module database, we can build a complex mechanical model to realize the simulation of the mechanical structure. Meantime, driver and the sensor modules are effective ways to connect Simmechanics with Simulink [21, 22].

As shown in Fig. 5, the model system can simulate the system controlled by the designed GUI. As shown in Fig. 5, there are six active joints, three passive joints and three fixed joints.

Figure 6 shows the module chart of the robot (Kawasaki ZX165U).

The following functions are included in the designed GUI (see Fig. 7):

(i) controlling the process of simulation;
(ii) forwarding and reviewing the information of joint angle;
(iii) obtaining the information of manipulator pose and then saving the data.

4.2 Verification of the kinematics analysis

Figure 8 shows the picture of the real robot ZX165U. In experiment, the end-effector of the robot goes through two different ways, among which one looks like the letter “W” while the other looks like an “S” (see Figs. 9 and 10).

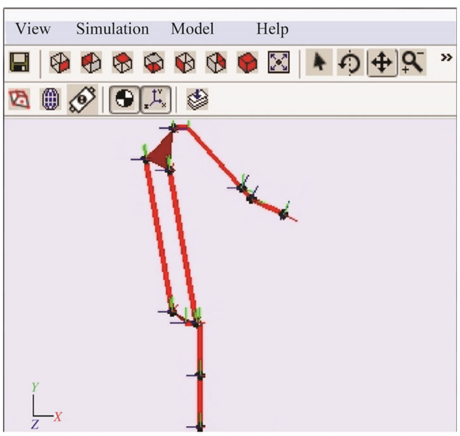

Fig. 5 Generated model in Simmechanics

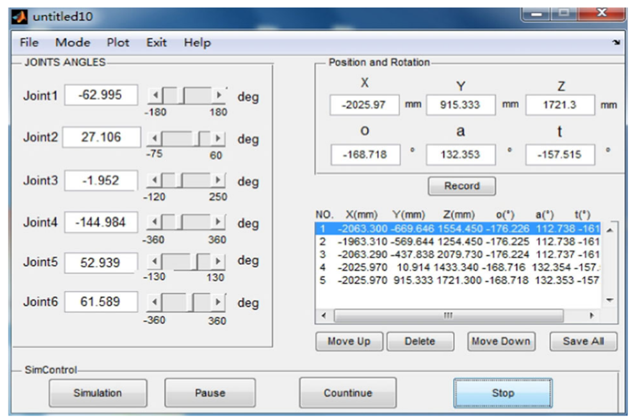

Fig. 7 GUI designed for controlling the robot model

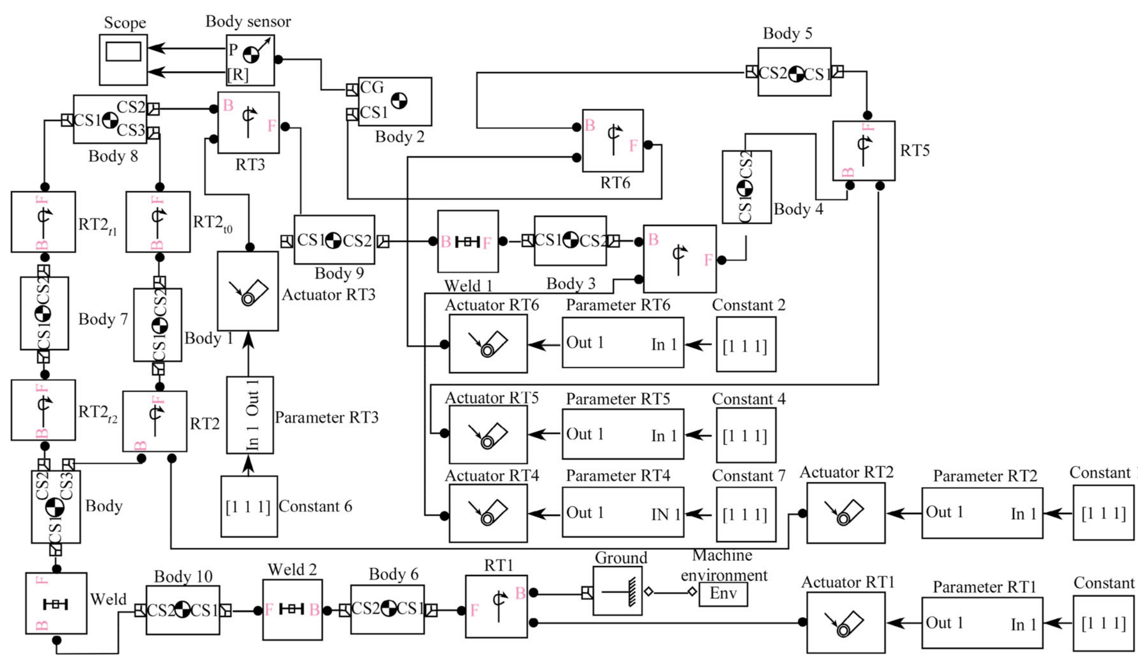

Fig. 6 Module chart of Kawasaki ZX165U robot

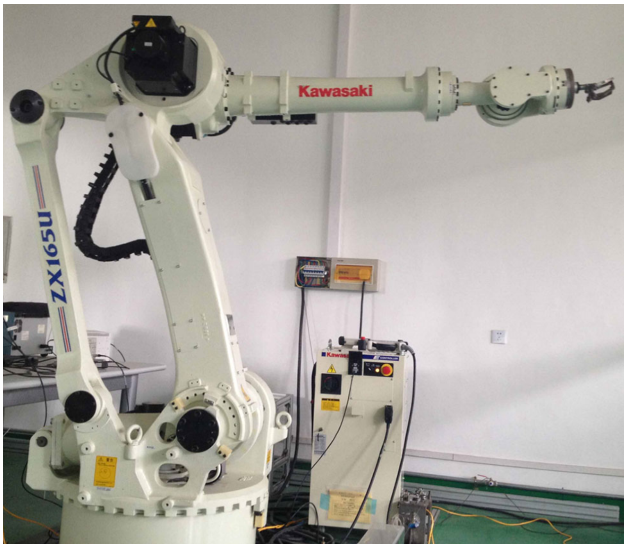

Fig. 8 Physical picture of the robot ZX165U

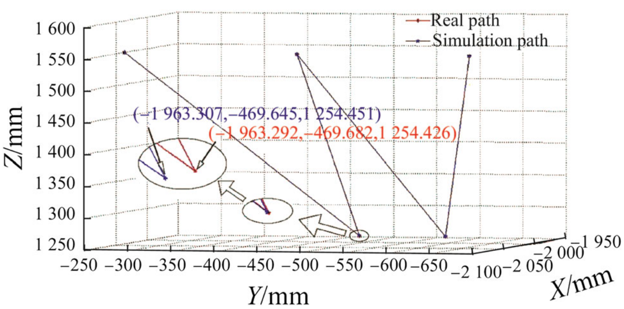

Fig. 9 Real and simulation "W" paths

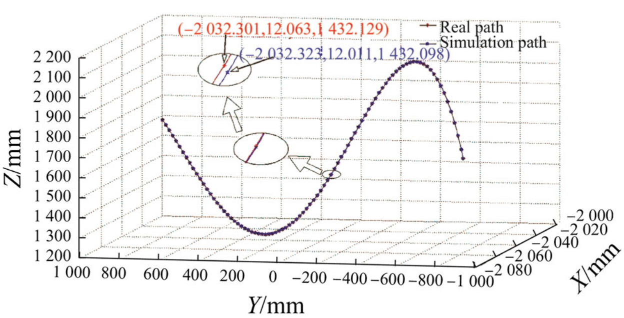

Fig. 10 Real and simulation "S" paths

The ZX165U robot can be driven to any arbitrary points in a reachable space as long as a set of appropriate values (joint angles or poses) are settled. In this experiment, five groups of data about points which indicate joint angles are put into the controller. Then the controller controls the robot to pass through these five points by linear interpolation (see Fig. 9) and curve interpolation (see Fig. 10). During this process, the pose and position of manipulator can be obtained at each corresponding point from teaching pendant. Then we let the robot model follow the same process by using the same data of 5 points mentioned above, but this time we use GUI to input data. Intuitively, the paths are drawn in a 3D coordinate system which only involves position values of robot but does not involve pose data. Figure 10 indicates the reverse.

From Figs. 9 and 10, it can be apparently seen that the actual path matches the simulation path within a certain range of minor errors. These minor errors cannot be noticed unless the paths are magnified by many times. As a matter of fact, the accuracy is already close to 0.02 mm, as shown in Tables 1 and 2.

We selected five arbitrary sets of data from process above and put all information in Table 1. Table 2 shows the data indicating inverse kinematics that are obtained in different ways. When the real and simulation robots move to the same designated pose and position, the data of their joint angles will be recorded. In Tables 1 and 2, "r-" and "s-" stand for words "real" and "simulation" respectively.

In Table 1, the mean error between simulation result and actual result is 0.0206 mm with the maximum error of 0.037 mm. Specifically, the position errors are 0.0258 mm, 0.0218 mm and 0.0142 mm corresponding to *X*, *Y* and *Z*. Such precision can satisfy any industrial requirement. *O*, *A* and *T* stand for *X*, *Y*, *Z* Euler angles, respectively. Furthermore, the pose error is almost negligible. Actually, we can never see the robot moving when it is shifted by a tiny distance. In Table 2, the mean error is 0.0011° by rough calculation with the wrong data—No.5 without JT4. It means that the model robot can reach a certain point within an acceptable error range (tiny error is incognizable). Just as mentioned in the previous section, the kinematics analysis is absolutely correct and can be proved by the comparison analysis of the data.

5 Conclusions

This paper analyzes and verifies the kinematics characteristic (translation motion) of a new-type robot with a mixed hinge structure. On the basis of that, the kinematic analysis can be easily carried out. Then the kinematic equation is established and solved with homogeneous transformation theory. The robot model built with kinematic equation solution can be used for simulation and acquire the simulation data via a designed GUI. Five groups of these data are selected, analyzed and compared. The error between real data and simulation data is calculated through the analysis. As shown in Tables 1 and 2, the errors are slight, which means that the simulation of the model can absolutely meet the actual requirement. Furthermore, the correctness of kinematics analysis is proved on the basis of the appropriate data analysis. This article hopes to provide some inspiration for those who are studying or going to study this kind of robot with a hybrid hinge structure.

Table 1 Values of the end-effector pose calculated from six angles (forward kinematics)

No.		JT1 *X*	JT2 *Y*	JT3 *Z*	JT4 *O*	JT5 *A*	JT6 *T*
1	Angles/(°)	−109.485	22.272	−14.039	−237.419	17.240	170.801
	r-pose/mm	−2 063.292	−669.681	1 554.426	−176.225	112.738	−161.616
	s-pose/mm	−2 063.300	−669.646	1 554.450	−176.226	112.738	−161.617
2	Angles/(°)	−107.587	21.784	−28.428	−291.437	13.683	225.816
	r-pose/mm	−1 963.292	−569.681	1 254.426	−176.224	112.738	−161.616
	s-pose/mm	−1 963.310	−569.644	1 254.450	−176.225	112.738	−161.616
3	Angles/(°)	−102.885	17.210	7.830	−196.067	31.841	125.679
	r-pose/mm	−2 063.292	−437.841	2 079.731	−176.224	112.737	−161.616
	s-pose/mm	−2 063.300	−437.838	2 079.730	−176.224	112.737	−161.615
4	Angles/(°)	−88.649	17.809	−17.936	−158.899	26.680	84.877
	r-pose/mm	−2 025.976	10.885	1 433.336	−168.714	132.354	−157.510
	s-pose/mm	−2 025.970	10.914	1 433.340	−168.716	132.345	−157.511
5	Angles/(°)	−62.995	27.106	−1.952	−144.984	52.939	61.589
	r-pose/mm	−2 025.990	915.327	1 721.282	−168.716	132.353	−157.514
	s-pose/mm	−2 025.970	915.333	1 721.300	−168.718	132.353	−157.515

Table 2 Angles of six joints calculated from the end-effector pose (inverse kinematics)

No.		JT1 *X*	JT2 *Y*	JT3 *Z*	JT4 *O*	JT5 *A*	JT6 *T*
1	Pose/mm	2 025.976	477.106	1 244.825	−168.715	132.355	−157.511
	r-angle/(°)	−74.670	24.682	−24.595	−135.562	28.219	53.006
	s- angle/(°)	−74.668	24.682	−24.595	−135.562	28.208	53.008
2	Pose/mm	−2 063.293	−835.524	1 689.418	−176.225	112.737	−161.616
	r-angle/(°)	−113.908	24.153	−7.343	−229.340	24.738	163.047
	s- angle/(°)	−113.909	24.153	−7.343	−229.342	24.738	163.049
3	Pose/mm	−1 963.292	−369.681	1 254.426	−176.225	112.738	−161.615
	r-angle/(°)	−101.471	19.467	−29.217	−311.372	9.473	243.137
	s- angle/(°)	−101.471	19.468	−29.217	−311.373	9.474	243.138
4	Pose/mm	−2 243.500	37.766	1 647.109	−176.225	112.738	−161.616
	r-angle/(°)	−88.546	24.849	−8.980	−160.582	14.643	87.526
	s- angle/(°)	−88.546	24.8498	−8.980	−160.581	14.643	87.525
5	Pose/mm	−2 256.349	−170.771	1 897.625	−175.823	101.698	−161.497
	r-angle/(°)	−94.344	24.235	0.035	−180.811	11.734	109.330
	s- angle/(°)	−94.345	24.236	0.035	−179.193	11.735	109.328

Acknowledgements This research was supported by the Key Scientific and Technological Project of Shanghai Science and Technology Commission (Grant No. 12111101004).

References

1. Bi LY, Liu LS (2012) 6-axis robot design and simulation based on simulationX. In: Yang DH (ed) Informatics in control, automation and robotics, vol 133. Springer, Heidelberg, pp 537–544
2. Song T, He YY, Wang P et al (2013) Kinematic analysis of series industrial robot with hybrid hinge structure. Mach Des Res 5:8–9
3. Fathi HG, Olivier C, Ruvinda G et al (2000) Modeling and set point control of closed-chain mechanisms: theory and experiment. IEEE Trans Control Syst Technol 8(8):801–815
4. Wang KS, Terje KL (1988) Structure design and kinematics of a robot manipulator. Robotica 6(4):299–309
5. Selig JM (2011) On the geometry of point-plane constraints on rigid-body displacements. Acta Appl Math 116:133–155
6. Suguru A, Masahiro S (2006) Human-like movements of robotic arms with redundant DOFs: virtual spring-damper hypothesis to tackle the Bernstein problem. In: Proceedings of IEEE international conference on robotics and automation, Orlando, May 2006
7. Choi HB, Konno A, Uchiyama M (2009) Closed-form forward kinematics solutions of a 4-DOF parallel robot. Int J Control Autom Syst 7(5):858–864
8. Pisla D, Gherman B, Vaida C et al (2012) Kinematic modeling of a 5-DOF hybrid parallel robot for laparoscopic surgery. Robotica 30(7):1095–1107
9. Gallardo-Alvarado J (2005) Kinematics of a hybrid manipulator by means of screw theory. Multibody Sys Dyn 14(3/4):345–366

10. Kuo SR, Yang YB (2013) A rigid-body-qualified plate theory for the nonlinear analysis of structures involving torsional actions. Eng Struct 47:2–15
11. Wang ZY, Zhao ZQ, Pang ZF et al (2011) Kinematics analysis and simulation of a new 3 degrees of freedom spatial robot mechanism composed by closed chain. In: The second international conference on mechanic automation and control engineering, Hohhot, July 2011
12. Wen GJ, Xu LH, He FL (2009) Offline kinematics simulation of 6-DOF welding robot. In: The 9th international conference on measuring technology and mechatronics automation, Zhangjiajie, April 2009
13. Xiao WL, Henning S, Torsten L et al (2011) Closed-form inverse kinematics of 6R milling robot with singularity avoidance. Prod Eng Devel 5:103–110
14. Wu Y, Cheng LH, Fan GF et al (2014) Inverse kinematics solution and optimization of 6-DOF handling robot. Appl Mech Mater 635–637:1355–1359
15. Gao JR, Wang YZ, Chen ZP (2014) Modeling and simulation of inverse kinematics for planar 3-RRR parallel robot based on SimMechanics. Adv Mater Res 898:510–513
16. Markus L (1994) Application of the general elimination method in robot kinematics. J Intell Rob Syst 11:109–116
17. Shi ZX, Ye MY, Luo YF et al (2011) The decoupled leading terms elimination algorithm and its application in inverse kinematic analysis of 5R robot. In: The international conference on computer science and service system, Nanjing, June 2011
18. Wang YS, Gai YX, Wu FY (2011) A robot kinematics simulation system based on OpenGL. In: The IEEE conference on robotics, automation and mechatronics, Qingdao, September 2011
19. Phung AS, Malzahn J, Hoffmann F et al (2011) Data based kinematic model of a multi-flexible-link robot arm for varying payloads. In: Proceedings of the the IEEE international conference on robotics and biomimetics, Karon Beach, December 2011
20. Toz M, Kucuk S (2008) Dynamics simulation toolbox for industrial robot manipulators. Comput Appl Eng Educ 18(2):319–330
21. Fatehi MH, Vali AR, Eghtesad M et al (2011) Modeling and control of 3-PRS parallel robot and simulation based on SimMechanics in MATLAB. In: 2nd international conference on control, instrumentation and automation, Shiraz, December 2011
22. Dean-Leon E, Nair S, Knoll A (2012) User friendly MATLAB-Toolbox for symbolic robot dynamic modeling used for control design. In: Proceedings of the IEEE international conference on robotics and biomimetics, Guangzhou, December 2012